DNA base-pair flipping with fluorescent perylenediimide pincers

ARTICLE *in* PHOTOCHEMICAL AND PHOTOBIOLOGICAL SCIENCES · JULY 2010

Impact Factor: 2.27 · DOI: 10.1039/c0pp00044b · Source: PubMed

4 AUTHORS, INCLUDING:

Mahesh Hariharan
Indian Institute Of Science Education and R…
45 PUBLICATIONS **843** CITATIONS
SEE PROFILE

Karsten Siegmund
Northwestern University
16 PUBLICATIONS **192** CITATIONS
SEE PROFILE

Frederick D Lewis
Northwestern University
319 PUBLICATIONS **9,207** CITATIONS
SEE PROFILE

This article is published as part of a themed issue of ***Photochemical & Photobiological Sciences*** in honour of

Jan Verhoeven

Guest edited by **Anthony Harriman**

Published in **issue 7, 2010**

Communication

Papers

DNA base-pair flipping with fluorescent perylenediimide pincers†‡

Tarek A. Zeidan,§ Mahesh Hariharan,¶ Karsten Siegmund and Frederick D. Lewis*

Received 3rd March 2010, Accepted 7th April 2010
First published as an Advance Article on the web 29th April 2010
DOI: 10.1039/c0pp00044b

The synthesis, structure, and electronic spectra of a series of DNA hairpins possessing two perylenediimide (PDI) base pair surrogates are reported. The PDI chromophores are located in opposite strands of the hairpin base pair domain opposite abasic sites and are either adjacent to each other or separated by a variable number of AT or GC base pairs. Molecular modeling of the conjugate having adjacent PDI chromophores shows that they adopt a slipped, π-stacked geometry with an angle of 40° between the PDI long axes. The electronic absorption, fluorescence, and circular dichroism of this conjugate are consistent with a stacked PDI structure. Conjugates having one or two GC base pairs between the PDI chromophores display spectra that are consistent with isolated PDIs. Conjugates having 1–4 AT base pairs have more complex spectra, suggestive of an equilibrium between base paired and flipped structures having stacked PDIs. Heating of the conjugates possessing isolated PDI chromophores results in base pair flipping. The free energy for PDI stacking is greater than that for a single AT base pair and comparable to that for a single GC base pair or two AT base pairs.

Introduction

Opening of individual Watson–Crick base pairs plays an important role in DNA dissociation, modification, repair, and cleavage.[1] Base pair opening within canonical B-DNA occurs with typical opening times of 1–10 ms for AT and 5–50 ms GC, reflecting the formation of stronger GC *vs.* AT base pairs. Activation energies for complete opening of a base pair are in the range 10–20 kcal mol^{-1}. Free energies for partial GC and AT base pair opening obtained from umbrella sampling simulations in a double stranded $d(GA)_6 \cdot d(CT)_6$ duplex are *ca.* 7 and 11 kcal mol^{-1}, respectively.[2] The restriction endonuclease PspGI recognizes pentameric CC-NGG sequences, where N can be from either an AT or GC base pair.[3] Upon binding, the two bases comprising the central base pair are flipped into hydrophobic pockets. The selectivity for binding and flipping of AT *vs.* GC pairs is amplified in the cleavage process, resulting in million-fold specificity. Introduction of strain into a duplex structure can also result in base flipping.[4] For example, a partially flipped structure has also been reported for a GC base pair under internal torsional stress from an interstrand crosslink.[5] Molecular modeling of a mini-hairpin having a short tri(ethylene glycol) linker indicates that the adjacent base pair is partially flipped.[6]

Flipping of mismatched or chemically damaged base pairs is less energetically demanding than flipping of matched base pairs. Partially flipped structures have been reported for GC wobble pairs.[7] A number of repair enzymes selectively bind to sites containing mismatched and damaged base pairs and selectively flip a single base into an extrahelical binding site where excision or repair occurs.[8] Enzymes which chemically modify nucleobases also flip their target to an extrahelical position. A bis-acridine macrocycle has been observed to recognize abasic sites and mismatched base pairs by sandwiching an adjacent GC base pair and displacing a mismatched thymine into an extrahelical position.[9] Conjugates possessing two hydrophobic perylenediimide (PDI) chromophores in the same strand are reported to flip out a single intervening mismatched AN base pair (N = A, G, C or an abasic site) but not a canonical AT base pair.[10]

We report here that two PDI chromophores located on opposite strands in a DNA hairpin conjugate can flip single or multiple Watson–Crick base pairs which are located between the PDI chromophores. Intramolecular PDI–PDI stacking provides the thermodynamic driving force for base pair flipping. These studies are facilitated by the pronounced changes in PDI UV-visible, circular dichroism, and fluorescence spectra which occur upon conversion of isolated chromophores to ground state dimers. The ease of base pair flipping is dependent upon both the number and identity (AT *vs.* GC) of base pairs separating the PDI pincers.

Experimental

The DNA building block P was prepared and incorporated into oligonucleotide conjugates following the method of Wagner and Wagenknecht.[11] Conjugates were purified by HPLC and characterized by MALDI-TOF mass spectrometry (Table S1, ESI‡). UV-vis absorption measurements were made using a Perkin-Elmer Lambda 2 spectrometer equipped with a Peltier sample holder and a temperature programmer for automatically changing the temperature at the rate of 0.5 °C min^{-1}. Fluorescence spectra were recorded over the temperature range 5–95 °C with 5 °C increments using a Spex Fluoromax spectrofluorimeter equipped with a Quantum Northwest temperature controller. Circular dichroism

Department of Chemistry, Northwestern University, Evanston, IL, 60208-3113, USA. E-mail: fdl@northwestern.edu

† This article is published as part of a themed issue in appreciation of the many important contributions made to the field of molecular photophysics by Jan Verhoeven.

‡ Electronic supplementary information (ESI) available: MALDI-TOF mass spectral data (Table S1) and UV, CD, and fluorescence spectral data (Fig. S1, S2, and S3). See DOI: 10.1039/c0pp00044b

§ Present address: Alkermes, Waltham, MA, USA.

¶ Present address: School of Chemistry, Indian Institute of Science Education and Research-Thiruvananthapuram (IISER-TVM), India.

spectra were recorded over the temperature range 5–95 °C with 5 °C increments using a Jasco J-815 Spectrophotometer equipped with Peltier temperature controller as previously described.[6] Solutions of the appropriate hairpin conjugates in TE buffer (0.2 M Tris, 0.02 M EDTA, pH 7.4) and NaCl (0.1 M) were annealed at 100 °C for 5 min and cooled slowly to room temperature prior to spectral measurements. Concentrations of conjugates for all spectroscopic studies were *ca.* 6–12 μM, which provides an absorbance of *ca.* 0.3–0.5 at 504 nm in a 0.5 cm path-length quartz cell having a volume of 1.0 ml. Concentrations were estimated using the reported molar absorbance of P in DMSO solution (60 250),[11] assuming that PDI association results in only minor changes in the integrated band intensities.

Results

Synthesis and structure

The PDI-modified conjugates shown in Chart 1 were synthesized by means of standard solid-supported synthesis with incorporation of the PDI base pair surrogate P opposite an abasic site, as previously described for hairpin conjugates containing a single P.[12] The surrogate P was prepared following the procedure of Wagner and Wagenknecht.[11] The conjugates were purified by HPLC and characterized by MALDI TOF mass spectrometry.

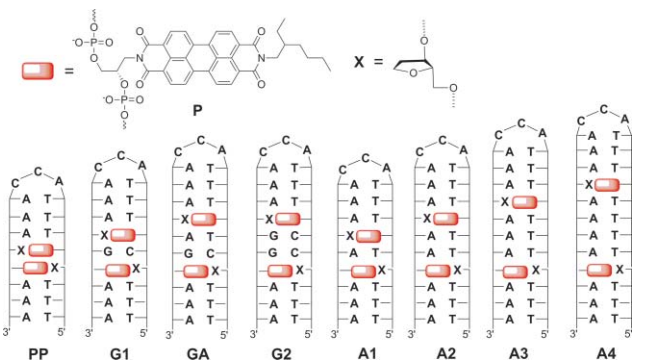

Chart 1 Structures of the base pair surrogate P, abasic site X, and hairpins studied.

The minimized structure of a duplex with the same structure as **PP** except for the absence of the CCA loop sequence is shown in Fig. 1. This structure was created with MacroModel[13] by inserting the PDI residues into a B-form DNA duplex in which one A-T base pair was removed from each strand. The resulting structure was first minimized with fixed positions for all atoms except for the PDI residues and neighboring atoms. Then the structure was minimized using the Amber force field[14] with implicit water followed by 600 ps of molecular dynamics under the same conditions with additional base planarity constraints on the terminal base pairs. Significant structural changes occur during the minimization process. The resulting mean plane-to-plane distances is 3.3 Å, the angle between PDI long-axes α is 40°, and the angles between these axes and the vector connecting the PDI centers β and β' are 70° and 75°.

UV-vis absorption spectra

The long-wavelength region of the UV-vis spectra of conjugates **PP**, **G1**, and **G2** are shown in Fig. 2. The spectra are normalized to

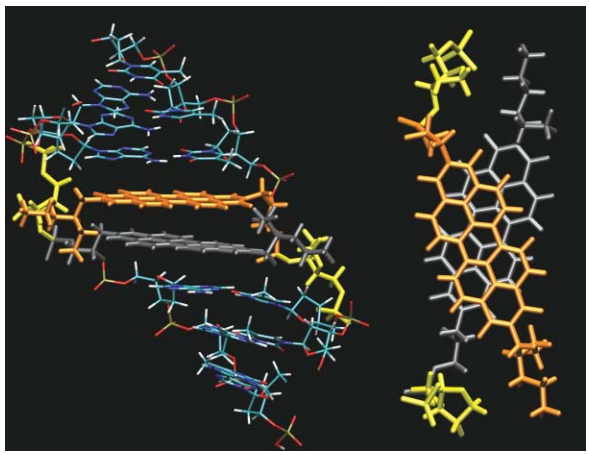

Fig. 1 Minimized structure for conjugate **PP** with CCA hairpin loop removed for ease of calculation: (left) viewed from side and (right) view of PDI dimer from above. PDI chromophores are in orange and grey and abasic sites are in yellow.

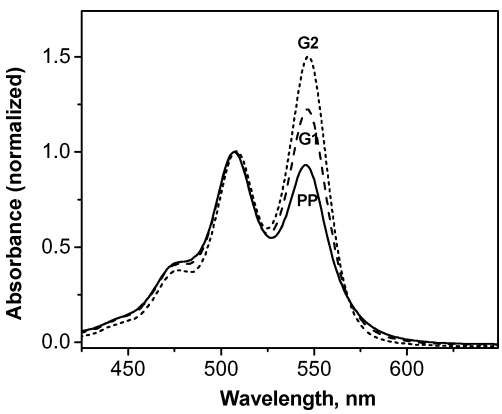

Fig. 2 UV-Vis spectra of **PP**, **G1**, and **G2** normalized for equal absorption at 505 nm. Solutions contain *ca.* 7 μM conjugate in TE buffer with 0.1 M NaCl.

provide equal absorbance for the second vibronic band at 505 nm. The normalized spectra have similar integrated band areas. The spectra of **G2** and **GA** (not shown) have $A^{0,0}/A^{0,1}$ band intensity ratios of 1.45 and 1.40 at 5 °C (Table 1), respectively, similar to those for other DNA–PDI conjugates possessing isolated PDI chromophores.[12,15] The ratio for conjugate **PP** at 5 °C is 0.85, smaller than that for monomeric PDI, but somewhat larger than the value of ~0.60 for PDI dimers that adopt sandwich-like geometries.[15,16] The spectra of **G1** (Fig. 2) and the conjugates **A1**–**A4** display $A^{0,0}/A^{0,1}$ band intensity ratios intermediate between those for **PP** and **G2** (Table 1).

The 260 nm band intensities for all of the conjugates increase upon heating, as expected for the occurrence of base-pair dissociation and de-stacking.[17] Only in the case of **G2** is a well defined melting transition observed (Fig. S1a, ESI‡), providing a base-pair melting temperature of 62 °C. The temperature dependence of the $A^{0,0}/A^{0,1}$ band intensity ratios for all of the conjugates are shown in Fig. S1a,b (ESI‡). $A^{0,0}/A^{0,1}$ thermal profiles obtained for heating and cooling display only minor hysteresis, indicative of reversible temperature-induced changes in conformation. The $A^{0,0}/A^{0,1}$ ratio for **PP** increases slightly from 0.85 to 0.95 upon heating from

Table 1 UV-Vis, circular dichroism and fluorescence data for the conjugates in Chart 1

Conjugate[a]	$A^{0,0}/A^{0,1}$ [b]	T_M, $A^{0,0}/A^{0,1}$ [c]	θ/mdeg[d]	T_M CD[e]	I_{550}/I_{665} [f]	T_{max} I_{fex} [g]
PP	0.85 (0.96)	[h]	+33	[h]	2.4	27
G1	1.19 (1.10)	32	–1.7	[h]	12	[h]
GA	1.40 (1.15)	46	–2.7	[h]	12	[h]
G2	1.45 (0.95)	61 (62)	–2.9	[h]	13	[h]
A1	1.0 (0.86)	13	+1.9	[h]	4.0	15
A2	1.20 (0.95)	29	–11.4	25	5.5	25
A3	1.25 (0.90)	31	–12.3	35	3.5	40
A4	1.28 (0.93)	45	+5.0	40	3.2	45

[a] Conjugate structures provided in Chart 1. [b] Ratio of intensities of the two longest wavelength absorption band intensities at 5 °C. Values in parentheses are the ratios at 95 °C. [c] Derivative of a plot of $A^{0,0}/A^{0,1}$ *vs.* temperature (Fig. S1a,b). Value in parentheses is the derivative of a plot of A^{260} *vs.* temperature for **G2**. [d] Rotational strength and sign of the longest wavelength CD band. [e] Derivatives of plots of CD rotational strength *vs.* temperature (Fig. S2). [f] Ratios of monomer/dimer fluorescence band maxima at 20 °C. [g] Temperatures at which the dimer fluorescence attains maximum intensity (Fig. S3). [h] Values cannot be determined from spectral data.

5 to 95 °C. The ratios for the other conjugates decrease upon heating, indicative of increased PDI–PDI association upon base pair melting. The derivatives of these plots provide the values of T_M reported in Table 1. In the case of **G2** similar T_M values are obtained from the 260 nm and $A^{0,0}/A^{0,1}$ data. The values of T_M increase for the series **G1** < **GA** < **GG** and **A1** < **A2** < **A3** < **A4** as expected for increased stability of the base pair domain separating the PDI chromophores. The low value for **A1** indicates that its single A-T base pair is largely dissociated at 20 °C; whereas the values for **G1**, **A2**, and **A3** are consistent with significant populations of base-paired conformations at 20 °C. The minimum values of $A^{0,0}/A^{0,1}$ band intensity ratios at high temperature are also reported in Table 1and lie in the range 0.86–1.15.

Circular dichroism spectra

The circular dichroism spectrum of **PP** (Fig. 3a) displays a strong positive bisignate signal at long-wavelengths characteristic of exciton coupling between the PDI chromophores.[18] This spectrum is similar in sign and band shape to the EC-CD spectrum reported by Baumstark and Wagenknecht for a duplex possessing two PDI chromophores opposite abasic sites.[19] The positive sign of the EC-CD spectrum of **PP** is consistent with incorporation of the PDI dimer within the right-hand helical structure of a DNA duplex base pair domain.[20] The CD spectra of the other PDI conjugates are shown in Fig. 3a,b and the sign and intensity of their long-wavelength CD bands are reported in Table 1. These conjugates have weaker long-wavelength CD bands than **PP** and signs that are either positive (**A1** and **A4**) or negative.

The CD spectra of the conjugates are strongly temperature dependent, as shown for **A2** in Fig. 4. In the case of **PP** the intensities of the 286 and 672 nm bands display a similar continuous decrease in intensity with increasing temperature. In the cases of **A2–A4** the derivatives of plots of the band intensity *vs.* temperature (Fig. S2, ESI‡) have maxima or minima similar to the T_M values obtained from the UV $A^{0,0}/A^{0,1}$ band intensity ratios (Table 1). The intensity of the 551 nm bands for the other conjugates are too weak to provide reliable CD melting curves.

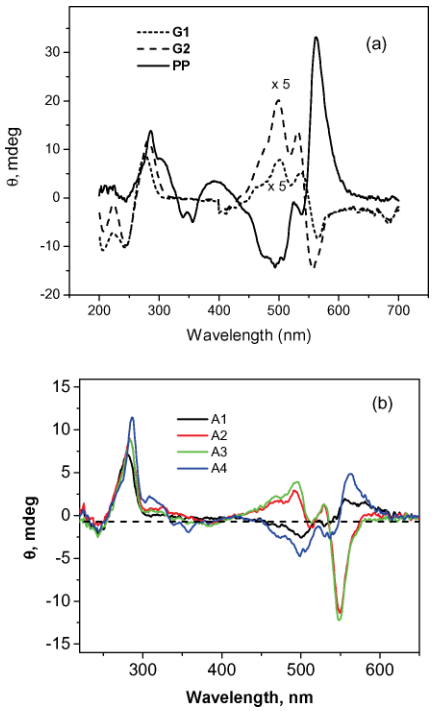

Fig. 3 Room temperature CD spectra of (a) PP, G1 and G2; (b) A1, A2, A3 and A4. Solutions contain *ca.* 7 μM conjugate in TE buffer with 0.1 M NaCl.

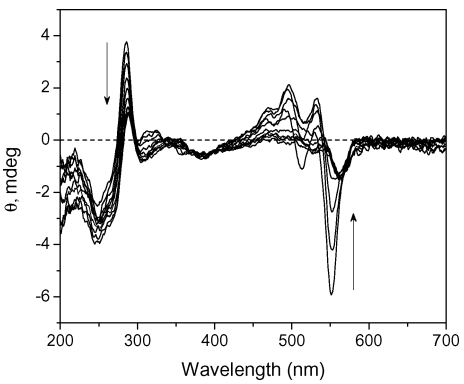

Fig. 4 Temperature-dependent CD spectra for **A2** from 5 to 95 °C in 10 °C increments. Arrows indicate spectral changes with increasing temperature. Solution contains *ca.* 7 μM conjugate in TE buffer with 0.1 M NaCl.

Fluorescence spectra

The fluorescence spectra for conjugates **PP**, **G1**, and **A1** normalized for equal intensity of their short-wavelength bands are shown in Fig. 5. The spectrum of **G1** is similar to that of other conjugates containing isolated PDI chromophores.[12] The long-wavelength maximum which is prominent in the spectrum of **PP** and to a lesser extent in **A1** is assigned to the PDI excited dimer or excimer. The I_{551}/I_{665} band intensity ratios for the conjugates are reported in Table 1. The ratios for **G1**, **GA**, and **G2** are characteristic of the PDI monomer.[15,16] The ratios for the other conjugates are between 2.4 and 5.5, indicative of variable amounts of PDI monomer and dimer emission.

The fluorescence spectra of the conjugates **PP** and **A1–A4** are strongly temperature dependent. As shown in Fig. 6 for **A3**, the

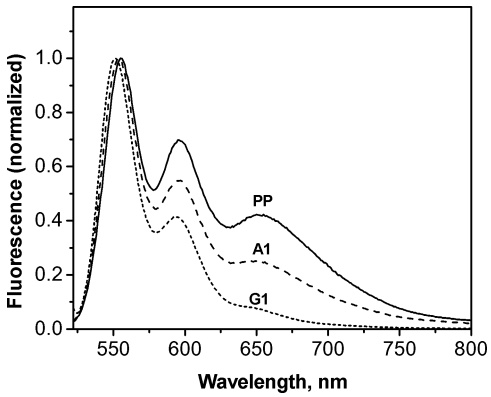

Fig. 5 Fluorescence spectra for **PP**, **A1** and **G1**. Solutions contain *ca.* 7 μM conjugate in TE buffer with 0.1 M NaCl.

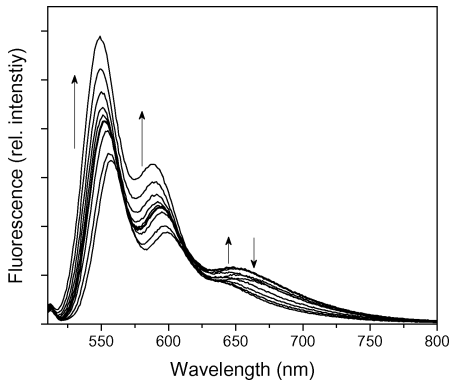

Fig. 6 Temperature-dependent fluorescence spectra of **A3** from 15 to 95 °C in 10 °C increments. The intensity of the short-wavelength bands increase continuously with increasing temperature; whereas the intensity of the long-wavelength band increases to a temperature of *ca.* 40 °C and then decreases with further increase in temperature. Solution contains *ca.* 7 μM conjugate in TE buffer with 0.1 M NaCl.

intensity of the two shorter wavelength bands attributed to the PDI monomer increase continuously with increasing temperature; whereas the intensity of the long wavelength band attributed to the dimer first increases with temperature and then decreases with a further increase in temperature. Plots of the temperature dependence of the 650 nm fluorescence intensity for **PP** and **A1–A4** are shown in Fig. S3 (ESI‡) and values of T_{max}, the temperature at which the dimer band reaches its maximum intensity, are reported in Table 1. These values are in good agreement with the values of T_M obtained from the $A^{0,0}/A^{0,1}$ band intensity ratios and 551 nm CD band intensities, where these values are available. The intensities of the 650 nm fluorescence of **G1**, **GA**, and **G2** are too weak to permit similar analysis of their temperature dependence.

Discussion

Structure and electronic spectra of PP

The selection of **PP** as the parent conjugate for the present study was based on the expectation that it would form a base-paired structure at room temperature but that base pair dissociation would occur upon moderate heating. Thus the effect of introduction of one or more base pairs between the PDI chromophores on hairpin stability should be largely determined by the central region of the conjugate encompassing the PDI chromophores and the intervening base pairs, rather than the short base-pair domains on either side of this central region. Molecular modeling of **PP** lacking the CCA hairpin loop (Fig. 1) indicates that the PDI chromophores adopt an approximately parallel sandwich-type structure with an average plane-to-plane distance of 3.3 Å, similar to the average base-pair stacking distance in DNA and distances calculated for the PDI gas phase dimer.[21–23] The calculated angle α between PDI long axes is 40°, somewhat larger than the values of $\alpha = 30°$ obtained from quantum mechanical calculations for the gas phase PDI dimer and $\alpha = 20°$ obtained by minimization of the structure calculated for the PDI-linked hairpin dimer.[15] The larger angle plausibly results from non-bonded interactions between the large *N*-alkyl groups in the base pair surrogate P (Chart 1) and the opposite strand. The centers of the PDI chromophores in our calculated structure are offset, unlike the aligned structures calculated for the gas phase dimer. The resulting values for the angles β and β' between the vector connecting the PDI centers and the PDI long axes are 70 and 75°, smaller than the value of $\beta = 90°$ calculated for the gas phase PDI dimer.[21] The slipped geometry presumably is a consequence of the conformational requirements of both the DNA backbone and the large hydrophobic *N*-alkyl substituents. We would caution that the removal of the *N*-alkyl groups, as done previously for the purposes of molecular modeling,[19] could provide inaccurate minimized structures.

We had expected that the electronic spectra of conjugate **PP** would be similar to those of other PDI dimers, such as the rigid dimer studied by Giaimo *et al.*[16] and the hairpin dimer formed by a PDI-linked hairpin.[15] The EC-CD spectrum of **PP** (Fig. 3a) displays a strong positive band, consistent with both the location of the PDI dimer within the right hand helical environment of a B-DNA structure[20] and the large dihedral angle between the PDI electronic transition dipoles (*vide infra*).[24] However, the UV spectrum of **PP** displays a larger $A^{0,0}/A^{0,1}$ band intensity ratio than that expected for a sandwich-type PDI dimer (0.85 *vs.* 0.6). We suspect that the low $A^{0,0}/A^{0,1}$ band intensity ratio is a consequence of the slipped geometry and the large value of α for the PDI dimer in **PP** (Fig. 1). According to the calculations of Seibt *et al.* this geometry should result in weaker exciton coupling than that for better aligned sandwich geometries.[22]

The fluorescence spectrum of **PP** (Fig. 5) displays a larger monomer/dimer intensity ratio than would be expected for a PDI dimer. Interpretation of the I_{551}/I_{665} band intensity ratios is complicated by several factors, including the low total quantum yields for both monomer and dimer fluorescence from PDI conjugates. The total fluorescence quantum yields reported for a PDI hairpin monomer and dimer are *ca.* 10^{-3}.[15] Even lower values are observed for PDI hairpins having a proximal G base, as a consequence of more efficient electron transfer quenching of both PDI monomer and dimer by G *vs.* A.[12,25] An additional complicating factor is the much weaker inherent fluorescence of the PDI dimer *vs.* monomer. For example, the quantum yields reported by Giaimo *et al.* for a *N*,*N*-dialkylperylene-diimide monomer and rigid dimer in chloroform are 0.98 and 0.02, respectively.[16] Relaxation of the Franck–Condon dimer excited state to the fluorescent excimer state is proposed to require geometric relaxation with parallel alignment of PDI transition dipoles.[26] Such changes may be inhibited by the geometric constraints imposed by the duplex

structure for **PP** (Fig. 1). Finally, monomer fluorescence from PDI foldamers having poly(ethylene glycol) linkers has been attributed to excimer dissociation to yield the locally excited singlet state.[27] In view of these several possible sources of monomer fluorescence from **PP**, we would caution against the use of monomer/dimer fluorescence ratio as the sole indicator of ground state PDI-PDI separation or association.

Electronic spectra of the base-pair separated conjugates

The electronic spectra of **G2** and **GA** are indicative of structures in which the two PDI chromophores are separated by intact base pairs at room temperature. Their $A^{0,0}/A^{0,1}$ absorption band intensity ratios at 5 °C (Table 1) are similar to those for single PDI chromophores in DNA conjugate structures.[12] The absence of dimer fluorescence is also consistent with the presence of intact GC base pairs (Fig. 5). The $A^{0,0}/A^{0,1}$ band intensity ratio for **G1** is smaller than that of **G2** or **GA**; however, **G1** displays only monomer fluorescence. Its $A^{0,0}/A^{0,1}$ band intensity ratio plausibly is reduced by exciton coupling, which is strongly distance dependent and thus may not be significant for **G2**.[17]

Interpretation of the electronic spectra of the conjugates **A1–A4** is less straight-forward than is the case for **G1** or **G2**. The $A^{0,0}/A^{0,1}$ absorption band intensity ratio for **A1** is smaller than that for **G1** and the ratios form **A2–A4** are smaller than those for **G2** or **GA** (Table 1). In addition, **A1–A4** all display significant dimer fluorescence. These observations suggest that none of the conjugates in this series have B-DNA structures with fully intact A-T base pairs separating the PDI chromophores. Rather, these conjugates appear to have significant populations of conformations in which the A-T base pair(s) are flipped out and the PDI chromophores are stacked. We note that the PDI dimer linked by a single-strand DNA oligomer studied by Wang *et al.* has a value of $A^{0,0}/A^{0,1} = 1.10$ at 20 °C,[28] larger than those for either **PP** or **A1**. Thus a disordered PDI dimer need not have a value of $A^{0,0}/A^{0,1}$ as small as 0.6. Further information about base pair dissociation is provided by the temperature dependence of the electronic spectra, as discussed in the following section.

Additional information about the structures of the PDI–PDI conjugates possessing intervening base pairs is provided by the sign and intensity of their EC-CD spectra. We previously reported that the sign and intensity of EC-CD spectra for stilbenedicarboxamide chromophores separated by a variable number of A-T base pairs are dependent upon both the vector distance between the planes of the chromophores R_{ij} and the angle θ between the electronic transition dipole moments μ_i and μ_j, which are long-axis polarized.[29,30] This dependence can be described by the simplified relationship in eqn (1) when the R_{ij} is perpendicular to and longer than μ_i and μ_j. As a consequence of the $\sin(2\theta)$ dependence, the CD spectrum should have zero intensity when $\theta = 0$, 90, or 180° and have maximum intensity but opposite sign for angles of 45 and 135°.

$$\Delta\varepsilon \approx \pm \frac{\pi}{4\lambda} \mu_a \mu_d R_{da}^{-2} \sin(2\theta) \quad (1)$$

The low intensities of the CD signals for **A1** and **G1** indicate that either the angle between their long axes is near 0° or 90° or that they have similar concentrations of conformations with positive and negative angles, as is the case for a PDI-linked hairpin dimer.[15] The stronger and sharper spectra observed for **G2** and **A2** indicate ordered structures. Their negative sign is consistent with an increase in the angle between PDI long axes upon interposition of two base pairs between PDI chromophores, which should increase the angle α between PDI chromophores from *ca.* 40° in **PP** to >90° in **G2** or **A2**. The similar sign and intensity of the EC-CD bands for **A3** and **A2** and the weaker intensity and change in sign for **A4** are also consistent with the effect of added base pairs predicted using eqn (1).

Interpretation of the fluorescence spectra of **A1–A4** is complicated by the same factors as encountered in the case of **PP**. Conjugates having intact base pair domains would be expected to exhibit only monomer fluorescence, as is the case for **G1**, **GA**, and **G2** (Table 1). The fluorescence spectra of conjugates **A1–A4** have I_{550}/I_{665} band ratios intermediate between the values for **PP** and **G1**. While these ratios would appear to be indicative of the presence of both stacked and unstacked conformations, we would caution against over-reliance on these ratios in support of a structural paradigm.

Temperature-dependent behavior

Increasing temperature is expected to effect base pair melting in our conjugates. The hypochromism associated with dissociation of the two short base pair domains does not result in well-defined 260 nm UV thermal dissociation profiles, except in the case of **G2** (Fig. S1a). For all of the conjugates except **PP**, heating results in a decrease in the $A^{0,0}/A^{0,1}$ UV band intensity ratios (Fig. S1). This decrease is attributed to dissociation of the base pair region between the PDI chromophores which leads to increased intramolecular PDI association. The derivatives of the $A^{0,0}/A^{0,1}$ UV band intensity ratio plots provide the values of T_M reported in Table 1. These values increase with increasing number of base pairs and upon replacement of AT with GC base pairs, as expected for B-DNA base pair thermal opening.[2] The low value of T_M for **A1** indicates that its single AT base pair is largely dissociated at room temperature.

In the case of **PP** the $A^{0,0}/A^{0,1}$ UV band intensity increases slightly with increasing temperature (Fig. S1). This increase can be attributed to a decrease in the strength of exciton coupling upon base pair melting resulting from an increase in conformational mobility. It is interesting to note that the value of $A^{0,0}/A^{0,1}$ at high temperature for most of the conjugates is *ca.* 0.95, similar to the value reported by Wang *et al.* for two PDI chromophores connected by a disordered single strand oligonucleotide at 90 °C.[28] The structures of our melted hairpins plausibly resemble that proposed by these workers for their single strand intramolecular dimer.

The derivates of the CD melting curves for the long-wavelength CD bands of conjugates **A2–A4** (Fig. S2) provide values of T_M similar to those obtained from the $A^{0,0}/A^{0,1}$ absorption band intensity ratios for these conjugates (Table 1). Loss of CD band intensity is attributed to base pair melting and the formation of disordered PDI dimers having similar populations of conformations having positive and negative values of α. Thus the temperature dependence of the $A^{0,0}/A^{0,1}$ absorption band intensity ratios and the CD band intensity are reporters of the same base-pair dissociation process. The CD band intensity for **PP** decreases continuously with increasing temperature, consistent

with gradual change from an ordered (Fig. 1) to disordered conformation without the transition attributed to dissociation of the intervening base pairs in **A2–A4**. The CD intensities of the other base-pair separated conjugates decrease with increasing temperature; however, their room temperature intensities are too low to permit estimation of a melting temperature.

The dimer fluorescence intensities of the conjugates **PP** and **A1–A4** first increase and then decrease with increasing temperature. The absence of measurable dimer fluorescence for the GC containing conjugates precludes a similar analysis. The maximum intensity of the dimer fluorescence bands of **A1–A4** (T_{max}, Table 1) are similar to the values of T_M determined from the temperature dependence of both their $A^{0,0}/A^{0,1}$ absorption band intensity ratios and their CD band intensities. The increase in intensity at low temperatures for **A1–A4** is attributed to changes in hairpin conformation which permit formation of an intramolecular dimer. The magnitude of these changes as well as the values of T_{max} increase as the number of AT base pairs increases. These changes are consistent with an equilibrium between base-paired and flipped out structures which is dependent upon the number of AT base pairs. The modest increase in dimer fluorescence intensity for **PP** at low temperatures plausibly reflects a small barrier for relaxation of the Franck–Condon excited state to the relaxed excimer state, as suggested by Fink *et al.*[26] The decrease in intensity for both **PP** and **A1–A4** at higher temperatures is attributed to the change from ordered to disordered dimer structures.

The value of T_{max} ~ 27 °C for **PP** is higher than values of T_M or T_{max} for **A1** but slightly lower than the values for **G1** or **A2** and distinctly lower than values of T_M for **G2**, **GA**, **A3** or **A4**. Thus PDI–PDI association is capable of flipping a single AT base pair at room temperature. It is interesting to note that a single AT base pair but not an AN mismatch is sufficient to separate two PDI's located within the same strand of a duplex.[10] Evidently the energetics of base pair flipping are different for inter- *vs.* intrastrand PDI–PDI conjugates. We have estimated a free energy of *ca.* −5 kcal mol^{-1} for dimerization of a PDI-linked hairpin based on the equilibirum between monomer and dimer at 20 °C.[15] This value is similar to estimates for PDI dimers in organic solvents, but smaller than the calculated values of *ca.* 7 kcal mol^{-1} and 11 kcal mol^{-1} for partial flipping of AT and GC base pairs, respectively.[2] The structural context of conjugate **A1** and **G1** is clearly different than that of either the PDI-linked hairpin dimer or canonical B-DNA and thus the energetics of both PDI association and base pair flipping may well be different.

Conclusions

Duplex DNA can adapt to both external and internal stress by base pair flipping. We find that hydrophobic PDI chromophores incorporated into a hairpin structure as base pair surrogates can function as pincers for the flipping of AT or GC base pairs located between the PDI's. The free energy for PDI π-stacking in a DNA construct provides a driving force sufficient to flip an AT base pair at room temperature and a GC or two AT base pairs at somewhat higher temperatures. Base pair flipping is studied by temperature dependent UV-Vis, CD, and fluorescence spectroscopy. Isolated PDI chromophores can be readily identified by the characteristic monomer spectra. However, the analysis of fully and partially associated PDI chromophores is complicated by the appearance of spectra intermediate between those expected for isolated and associated PDI chromophores. Thus first order analysis of these spectra is not possible. We suspect that these complications result from dimer structures which are not well-stacked as a consequence of the conformational restrictions imposed by the hairpin backbone and by the large *N*-alkyl groups on the PDI chromophores.

Acknowledgements

This research was supported by a grant form the National Science Foundation, Collaborative Research in Chemistry for the project DNA Photonics (CHE-0628130).

Notes and references

1 M. Guéron and J. L. Leroy, in *Nucleic Acids and Molecular Biology*, ed. F. Eckstein and D. M. J. Lilley, Springer-Verlag, New York, 1992, pp. 1–22.
2 E. Giudice, P. Varnai and R. Lavery, Base pair opening within B-DNA: free energy pathways for GC and AT pairs from umbrella sampling simulations, *Nucleic Acids Res.*, 2003, **31**, 1434–1443.
3 R. H. Szczepanowski, M. A. Carpenter, H. Czapinska, M. Zaremba, G. Tamulaitis, V. Siksnys, A. S. Bhagwat and M. Bochtler, Central base pair flipping and discrimination by PspGI, *Nucleic Acids Res.*, 2008, **36**, 6109–6117.
4 S. Cocco and R. Monasson, Statistical mechanics of torque induced denaturation of DNA, *Phys. Rev. Lett.*, 1999, **83**, 5178–5181.
5 D. M. F. van Aalten, D. A. Erlanson, G. L. Verdine and L. Joshua-Tor, A structural snapshot of base-pair opening in DNA, *Proc. Natl. Acad. Sci. U. S. A.*, 1999, **96**, 11809–11814.
6 M. McCullagh, L. Zhang, A. H. Karaba, H. Zhu, G. C. Schatz and F. D. Lewis, Effect of loop distortion on the stability and structural dynamics of DNA hairpin and dumbbell conjugates, *J. Phys. Chem. B*, 2008, **112**, 11415–11421.
7 P. Varnai, M. Canalia and J. L. Leroy, Opening mechanism of G-T/U pairs in DNA and RNA duplexes: A combined study of imino proton exchange and molecular dynamics simulation, *J. Am. Chem. Soc.*, 2004, **126**, 14659–14667.
8 A. E. Wolfe and P. J. O'Brien, Kinetic mechanism for the flipping and excision of 1,N-6-ethenoadenine by human alkyladenine DNA glycosylase, *Biochemistry*, 2009, **48**, 11357–11369.
9 A. David, N. Bleimling, C. Beuck, J. M. Lehn, E. Weinhold and M. P. Teulade-Fichou, DNA mismatch-specific base flipping by a bisacridine macrocycle, *ChemBioChem*, 2003, **4**, 1326–1331.
10 D. Baumstark and H. A. Wagenknecht, Perylene bisimide dimers as fluorescent "Glue" for DNA and for base-mismatch detection, *Angew. Chem., Int. Ed.*, 2008, **47**, 2612–2614.
11 C. Wagner and H. A. Wagenknecht, Perylene-3,4:9,10-tetracarboxylic acid bisimide dye as an artificial DNA base surrogate, *Org. Lett.*, 2006, **8**, 4191–4194.
12 T. A. Zeidan, R. Carmieli, R. F. Kelley, T. M. Wilson, F. D. Lewis and M. R. Wasielewski, Charge-transfer and spin dynamics in DNA hairpin conjugates with perylenediimide as a base-pair surrogate, *J. Am. Chem. Soc.*, 2008, **130**, 13945–13955.
13 F. Mohamadi, N. G. J. Richard, W. C. Guida, R. Liskamp, M. Lipton, C. Caufield, G. Chang, T. Hendrickson and W. C. Still, MacroModel - an integrated software system for modeling organic and bioorganic molecules using molecular mechanics, *J. Comput. Chem.*, 1990, **11**, 440–467.
14 W. D. Cornell, P. Cieplak, C. I. Bayly, I. R. Gould, K. M. Merz, D. M. Ferguson, D. C. Spellmeyer, T. Fox, J. W. Caldwell and P. A. Kollman, A second generation force field for the simulation of proteins, nucleic acids, and organic molecules, *J. Am. Chem. Soc.*, 1995, **117**, 5179–5197.
15 M. Hariharan, Y. Zheng, H. Long, T. A. Zeidan, G. C. Schatz, J. Vura-Weis, M. R. Wasielewski, X. B. Zuo, D. M. Tiede and F. D. Lewis, Hydrophobic dimerization and thermal dissociation of perylenediimide-linked DNA hairpins, *J. Am. Chem. Soc.*, 2009, **131**, 5920–5929.
16 J. A. Giaimo, J. V. Lockard, L. E. Sinks, A. M. Scott, T. M. Wilson and M. R. Wasielewski, Excited singlet states of covalently bound, cofacial

dimers and trimers of perylene-3,4:9,10-bis(carboximide)s, *J. Phys. Chem. A*, 2008, **112**, 2322–2330.
17 C. R. Cantor and P. R. Schimmel, *Techniques for the Study of Biological Structure and Function*, W. H. Freeman, New York, 1980.
18 N. Berova and K. Nakanishi, in *Circular Dichroism*, ed. N. Berova, K. Nakanishi and R. W. Woody, Wiley-VCH, New York, 2000.
19 D. Baumstark and H. A. Wagenknecht, Fluorescent hydrophobic zippers inside duplex DNA: Interstrand stacking of perylene-3,4:9,10-tetracarboxylic acid bisimides as artificial DNA base dyes, *Chem.–Eur. J.*, 2008, **14**, 6640–6645.
20 L. van Dijk, P. A. Bobbert and F. C. Spano, Extreme sensitivity of circular dichroism to long-range excitonic couplings in helical supramolecular assemblies, *J. Phys. Chem. B*, 2010, **114**, 817–825.
21 A. E. Clark, C. Qin and A. D. Q. Li, Beyond exciton theory: A time-dependent DFT and Franck–Condon study of perylene diimide and its chromophoric dimer, *J. Am. Chem. Soc.*, 2007, **129**, 7586–7595.
22 J. Seibt, P. Marquetand, V. Engel, Z. Chen, V. Dehm and F. Würthner, On the geometry dependence of molecular dimer spectra with an application to aggregates of perylene bisimide, *Chem. Phys.*, 2006, **328**, 354–362.
23 F. Pan, F. Gao, W. Z. Liang and Y. Zhao, Nature of low-lying excited states in H-aggregated perylene bisimide dyes: results of TD-LRC-DFT and the mixed exciton model, *J. Phys. Chem. B*, 2009, **113**, 14581–14587.
24 N. Harada and K. Nakanishi, *Circular dichroic spectroscopy : exciton coupling in organic stereochemistry*, University Science Books, Mill Valley, CA, 1983.
25 R. Carmieli, T. A. Zeidan, R. F. Kelley, Q. Mi, F. D. Lewis and M. R. Wasielewski, Excited state, charge transfer and spin dynamics in DNA hairpin conjugates with perylenediimide hairpin linkers, *J. Phys. Chem. A*, 2009, **113**, 4691–4700.
26 R. F. Fink, J. Seibt, V. Engel, M. Renz, M. Kaupp, S. Lochbrunner, H. M. Zhao, J. Pfister, F. Würthner and B. Engels, Exciton trapping in π-conjugated materials: A quantum-chemistry-based protocol applied to perylene bisimide dye aggregates, *J. Am. Chem. Soc.*, 2008, **130**, 12858–12859.
27 J. J. Han, A. D. Shaller, W. Wang and A. D. Q. Li, Architecturally diverse nanostructured foldamers reveal insightful photoinduced single-molecule dynamics, *J. Am. Chem. Soc.*, 2008, **130**, 6974–6982.
28 W. Wang, W. Wan, H. H. Zhou, S. Q. Niu and A. D. Q. Li, Alternating DNA and π-conjugated sequences. Thermophilic foldable polymers, *J. Am. Chem. Soc.*, 2003, **125**, 5248–5249.
29 F. D. Lewis, X. Y. Liu, Y. S. Wu and X. B. Zuo, Stepwise evolution of the structure and electronic properties of DNA, *J. Am. Chem. Soc.*, 2003, **125**, 12729–12731.
30 F. D. Lewis, L. Zhang, X. Liu, X. Zuo, D. M. Tiede, H. Long and G. C. Schatz, DNA as helical ruler: Exciton-coupled circular dichroism in DNA conjugates, *J. Am. Chem. Soc.*, 2005, **127**, 14445–14453.

